

# **A Framework for Engineering Stress Resilient Plants Using Genetic Feedback Control and Regulatory Network Rewiring**

**Foo, M., Gherman, I., Zhang, P., Bates, D. & Denby, K.**

**Author post-print (accepted) deposited by Coventry University's Repository**

**Original citation & hyperlink:**

Foo, M, Gherman, I, Zhang, P, Bates, D & Denby, K 2018, 'A Framework for Engineering Stress Resilient Plants Using Genetic Feedback Control and Regulatory Network Rewiring', ACS Synthetic Biology, vol. 7, no. 6, 7, pp. 1553-1564.  
<https://dx.doi.org/10.1021/acssynbio.8b00037>

DOI 10.1021/acssynbio.8b00037

ESSN 2161-5063

Publisher: American Chemical Society

**This document is the Accepted Manuscript version of a Published Work that appeared in final form in ACS Synthetic Biology, copyright © American Chemical Society after peer review and technical editing by the publisher. To access the final edited and published work see <http://dx.doi.org/10.1021/acssynbio.8b00037>**

**Copyright © and Moral Rights are retained by the author(s) and/ or other copyright owners. A copy can be downloaded for personal non-commercial research or study, without prior permission or charge. This item cannot be reproduced or quoted extensively from without first obtaining permission in writing from the copyright holder(s). The content must not be changed in any way or sold commercially in any format or medium without the formal permission of the copyright holders.**

**This document is the author's post-print version, incorporating any revisions agreed during the peer-review process. Some differences between the published version and this version may remain and you are advised to consult the published version if you wish to cite from it.**

This document is confidential and is proprietary to the American Chemical Society and its authors. Do not copy or disclose without written permission. If you have received this item in error, notify the sender and delete all copies.

## **A Framework for Engineering Stress Resilient Plants using Genetic Feedback Control and Regulatory Network Rewiring**

Journal:	<i>ACS Synthetic Biology</i>
Manuscript ID	sb-2018-00037h.R1
Manuscript Type:	Article
Date Submitted by the Author:	25-Apr-2018
Complete List of Authors:	Foo, Mathias; University of Warwick Gherman, Iulia; University of Warwick Zhang, Peijun; University of Sheffield Bates, Declan; University of Warwick Denby, Katherine; University of York

SCHOLARONE™  
Manuscripts

**A Framework for Engineering Stress Resilient Plants using  
Genetic Feedback Control and Regulatory Network  
Rewiring**

Mathias Foo<sup>1,†</sup>, Iulia Gherman<sup>1,†</sup>, Peijun Zhang<sup>2</sup>, Declan G. Bates<sup>1\*</sup> and Katherine J. Denby<sup>3\*</sup>

- 1. Warwick Integrative Synthetic Biology Centre, School of Engineering, University of Warwick, Coventry CV4 7AL, United Kingdom
- 2. Department of Animal and Plant Sciences, University of Sheffield, Sheffield, S10 2TN, United Kingdom
- 3. Department of Biology and Centre for Novel Agricultural Products, University of York, York YO10 5DD, United Kingdom

<sup>†</sup> Joint first authors. \*Correspondence: d.bates@warwick.ac.uk, katherine.denby@york.ac.uk

**ABSTRACT**

Crop disease leads to significant waste world-wide, both pre- and post-harvest, with subsequent economic and sustainability consequences. Disease outcome is determined both by the plants' response to the pathogen and by the ability of the pathogen to suppress defense responses and manipulate the plant to enhance colonization. The defense response of a plant is characterized by significant transcriptional reprogramming mediated by underlying gene regulatory networks and components of these networks are often targeted by attacking pathogens. Here, using gene expression data from *Botrytis cinerea*-infected Arabidopsis plants, we develop a systematic approach for mitigating the effects of pathogen-induced network perturbations, using the tools of synthetic biology. We employ network inference and system identification techniques to build an accurate model of an Arabidopsis defense sub-network that contains key genes determining susceptibility of the plant to the pathogen attack. Once validated against time-series data, we use this model to design and test perturbation mitigation strategies based on the use of genetic feedback control. We show how a synthetic feedback controller can be designed to attenuate the effect of external perturbations on the transcription factor CHE in our sub-network. We investigate and compare two approaches for implementing such a controller biologically – direct implementation of the genetic feedback controller, and rewiring the regulatory regions of multiple genes - to achieve the network motif required to implement the controller. Our results highlight the potential of combining feedback control theory with synthetic biology for engineering plants with enhanced resilience to environmental stress.

**KEYWORDS:** plant synthetic biology, plant-pathogen interaction, synthetic gene circuits, feedback control, network rewiring, plant defense response

Unfavorable environmental conditions during the growth of crop plants can cause significant yield loss and reduction in quality. These conditions include abiotic stresses, such as drought and extreme temperature, as well as the biotic stresses of disease and herbivory. Climate change is driving increasingly unpredictable and variable weather, and bringing associated change in pathogen (and hence disease) prevalence and incidence.<sup>1, 2</sup> It is therefore important to develop crops that are resilient to varying conditions and able to maintain yield in suboptimal environments.<sup>3</sup> The introduction and/or removal of single genes via genetic engineering has led to plants with enhanced tolerance to particular abiotic and biotic stresses,<sup>4</sup> however, often such approaches have unintended consequences on other plant responses,<sup>5</sup> and in the case of disease resistance they may not be durable. Recent increased understanding of how plant responses to different environmental conditions are controlled and integrated, together with the development of systems biology approaches, has opened up the possibility of designing stress resilient crops using engineering principles. In this work, we have focused on transcriptional regulation, as transcriptional reprogramming is a significant component of plant stress responses<sup>6-8</sup> and a point of cross-talk between responses to different stresses.<sup>9</sup>

In this paper we focus on the regulation of the defense response induced in Arabidopsis by the fungal pathogen, *Botrytis cinerea*.<sup>10</sup> When pathogens infect plants, disease is the result of dynamic interactions between the two organisms. Pathogens secrete a range of proteins, small RNAs and metabolites to disrupt host defense and manipulate the extra- and intracellular environment to aid colonization.<sup>11-14</sup> This is thought to explain why some positive regulators of defense are downregulated during infection, for example expression of TGA3 decreases during *B. cinerea* infection of Arabidopsis, yet plants lacking TGA3 expression are more susceptible to this pathogen.<sup>10</sup> In this study, we use a control engineering approach to counteract such potentially pathogen-mediated perturbations of positive regulators of defense. Constitutive overexpression of such positive regulators would be an obvious approach, but this brings significant drawbacks; the positive regulator of defense may have other roles in the plant which are disrupted due to constitutively high levels of expression, and constitutive activation of plant defense responses is known to often impact on growth.<sup>15</sup> Our proposed approach, which seeks to dynamically respond to perturbations of expression over the time-course of infection, should overcome these drawbacks.

From the perspective of control engineering, this scenario can be naturally formulated mathematically as a disturbance attenuation problem. For such problems, control engineers have developed a variety of powerful theoretical tools and techniques that allow the design of feedback controllers that can attenuate the effects of external perturbations on the functioning of a system or network (see ref 16 and references therein). The application of

these tools to the analysis and design of complex biological networks is now attracting significant interest within the synthetic biology community.<sup>17, 18</sup> To date, however, the potential usefulness of such approaches for engineering more resilient plants has not been investigated.

Here, we explore how combining control engineering design tools<sup>19-21</sup> with synthetic biology techniques could be used to enhance resistance against *B. cinerea* in Arabidopsis by preventing downregulation of a positive regulator of defense during infection. We design and test our controller using a model of the Arabidopsis gene regulatory sub-network underlying the transcriptional response to *B. cinerea* infection. This network model is formulated using ordinary differential equations (ODEs) and constructed from experimental data using network inference and system identification techniques. It is then validated against different time-series transcriptome datasets capturing the response of the plant's regulatory network to pathogen attack. Simulation results show the capability of the proposed approach to significantly reduce the perturbation of a positive regulator of plant defense in response to infection. We propose a novel strategy for implementing the controller experimentally, which avoids the need for the incorporation of any exogenous synthetic control circuitry. This strategy is based on the insight that the network motif required for the controller can be implemented by rewiring the regulatory regions of existing genes in the plant's stress-response network. We show how this can be done through the addition of gene coding sequences under the control of alternative regulatory regions.

## RESULTS

**Inferring the regulatory sub-network containing a positive regulator of defense.** We previously generated a high-resolution time series of the Arabidopsis transcriptome during the first 48 hours after inoculation by the pathogen *B. cinerea*.<sup>10</sup> Nearly 10,000 genes were identified as being differentially expressed in infected leaves compared to mock-inoculated leaves, including 883 TFs (Supplementary File 1a). We used the time-series transcriptome data for the differentially expressed TFs as input for network inference algorithms, to generate causal directed network models of the regulatory events underlying changes in expression of these TF genes. The algorithms chosen for this purpose (GENIE3<sup>22</sup>, TIGRESS<sup>23</sup> and Inferelator<sup>24</sup>), were highly ranked in a recent assessment of network inference algorithms.<sup>25</sup> GENIE3 approaches network inference as a tree-based regression problem and came first in the DREAM4 *in silico* multifactorial network inference challenge.<sup>25</sup> Inferelator and TIGRESS both use feature selection and least angle regression to rank the potential regulators of a gene. The outputs from these three algorithms were used to generate a consensus network model, as a robust way of generating high confidence networks.<sup>26</sup> A threshold (edges  $\leq 10$  times the number of nodes) was applied to this

consensus network to limit it to 8,830 edges. Furthermore only the top three regulators of each node were kept based on the highest probability score. From this final network, we looked for sub-networks surrounding positive regulators of defense against *B. cinerea* that were downregulated during infection. This led us to focus on a 9-gene regulatory network, termed 9GRN (see Figure 2) containing the TF CHE, which includes predicted upstream regulators of CHE.

**CHE is a positive regulator of defense against *B. cinerea*.** Expression of the transcription factor (TF) *CCA1 HIKING EXPEDITION (CHE)* is downregulated during *B. cinerea* infection (ref 10 and Figure 1a). Rhythmic expression of *CHE* is clear in the mock-inoculated samples (reflecting the role of CHE within the circadian clock<sup>27</sup>) with downregulation due to infection beginning around 22 hours post inoculation. A mutant with significantly reduced expression of CHE, *che-1*,<sup>27</sup> shows increased susceptibility to *B. cinerea* compared to wildtype indicating CHE plays a positive role in defense against this pathogen (Figure 1b). In addition to *CHE*, two other genes in the 9GRN are important in defense against *B. cinerea*: *ORA59* and *at-ERF1*. *ORA59* is a positive regulator of defense<sup>28</sup> and *at-ERF1* is a negative regulator of defense (Figure S1).

**Validating edges in the 9GRN model.** To increase our confidence in the validity of the inferred 9GRN sub-network model, we used yeast-1-hybrid (Y1H), a partial Arabidopsis cistrome map<sup>29</sup>, and gene expression data from *RAP2.6L* overexpressors<sup>30</sup> to test regulation predicted by the model. A set of pair-wise Y1H had been carried out testing binding of 75 TFs to the promoter regions of 34 of the same TFs. Within this set, there were 4 edges in our model (*RAP2.6L* to *ANAC055*; *ANAC055* to *RAP2.6L*, *ANAC055* to *ORA59* and *at-ERF1* to *ORA59*) that had been tested. For two of these edges, strong binding was seen in the Y1H experiments; *RAP2.6L* could bind to the promoter of *ANAC055* and *at-ERF1* could bind to the promoter of *ORA59* (Figure S2). In addition, the Y1H data suggested two additional edges that were missing from our model (*RAP2.6L* to *ORA59*, and *ORA59* to *ANAC055*), however, expression data from *RAP2.6L* overexpressors<sup>30</sup> and knockout mutant of *ORA59*<sup>28</sup> do not show any evidence for these regulatory edges. Additional interactions in the 9GRN were verified using data from an Arabidopsis cistrome map.<sup>29</sup> The cistrome is the complete set of cis-elements or TF binding sites in an organism, and a partial map was generated by O'Malley et al.<sup>29</sup> using DNA affinity purification sequencing (DAP-seq) to identify TF binding sites for 349 TFs (including CHE, *ORA59*, *ANAC055* and *MYB51* from our network). This analysis revealed that *ANAC055* can bind to the promoters of *ORA59* and *RAP2.6L*. Finally, the *RAP2.6L* overexpressing mutant showed increased expression of *AT1G79150*, providing

evidence for this regulatory interaction.<sup>30</sup> Edges with supporting experimental data are shown in green in Figure 2.

**A validated dynamic model of the CHE regulatory sub-network.** The network inference algorithms used to infer the large consensus network model are able to predict regulatory relationships between the genes in the 9GRN but the type of regulation (i.e. activating or inhibiting) cannot be determined. Since these are essential features of any model that can be used for controller design, we next determined the direction of the regulatory edges in the 9GRN using standard four-step system identification techniques: data collection, model structure selection, parameter estimation and model validation (see chapters 1 and 7 of ref 31). Previous studies that utilized this technique to identify regulation types in GRNs used *linear* models<sup>31-33</sup>, and there is now strong evidence that the underlying dynamics of GRNs can be accurately described using such models (we define accurate as a model able to recapitulate experimental data within a single standard deviation of error).<sup>34, 35</sup> Moreover, as the model is subsequently to be used to design perturbation mitigation strategies, a linear model facilitates the use of linear control design techniques that are more established than their nonlinear counterparts. In system identification terminology, black box models refer to a set of ready-made models with no physical structure or biological interpretation. On the other hand, gray box models refer to models that are tailor-made given some prior information about the system. Since we have prior knowledge of the direction of regulation between the genes obtained from the inferred network above, we use a *linear gray box* model comprising nine ODEs (Equation 4 in the Methods section) for the 9GRN, and thus only need to identify the regulation type and dynamics within the 9GRN.

The values of the model parameters were estimated from the available mRNA time-series data<sup>10</sup> using a nonlinear least squares algorithm<sup>36, 37</sup> (Equation 5 in Methods section) and the estimated parameters are given in Table 3 in Methods section. As these mRNA time-series measurements are normalized using an intensity-dependent normalization method,<sup>38, 39</sup> the resulting measurements are dimensionless and are reported as relative expression. Figure 2 indicates the regulation types identified in the 9GRN sub-network, where positive and negative values of production rate given in Table 3 in the Methods section denote transcriptional activators and inhibitors respectively. In addition, all the estimated degradation rates had the expected negative sign, and had numerical values within the range expected.<sup>40</sup> We validated the dynamic model by comparing its response against another mRNA time-series data set (see Methods section) that was not used in the parameter estimation process as well as two mutant behaviors. As shown in Figures 3 and S3, the identified model is able to accurately predict the expression behavior of the network.



Additionally, the model shows good predictive capability against two mutant datasets (see Figure S4).

**Design of a feedback controller for perturbation mitigation.** As outlined above, our control objective is to employ feedback to prevent the reduction in *CHE* levels when the plant is subjected to pathogen attack. There are several frameworks available for designing genetic controllers.<sup>19, 21, 41</sup> In refs 19 and 41, the authors proposed and extended a framework for implementing an integral controller using a negative feedback of a two-promoter gene network. In ref 21, the authors analyzed the dynamics of gene regulation using frequency domain tools from control theory and proposed the implementation of a genetic phase lag controller. Here, we based our design on the framework proposed in Harris et al.<sup>21</sup>, where the proposed genetic controller is made up of a combination of genes and the regulatory relationships between them. In ref 21, these gene regulations are modeled using nonlinear Michaelis-Menten type functions and these functions are then linearized such that the controller design and analysis can be done using standard frequency domain methods. In this study, since we have used a linear model to describe the 9GRN, we also model the gene regulations in the controller using linear functions.

Figure 4a shows the genetic circuit diagram of the proposed feedback controller. The controller architecture is modified from the framework suggested in ref 21, whereby for the purposes of implementation in plants we replace the protease degradation component with a transcriptional inhibitor component. The modified circuit contains three genes and their associated proteins: genes *X*, *Y* and *E* giving proteins *X*, *Y* and *E*.

Let *X* denote an arbitrary gene that can be regulated by *E*, and its translated protein *X* denotes the TF that can regulate the *output gene*, *Y*, whose levels we ultimately want to control. *E* denotes the protein whose function is to regulate gene *X* and calculate the *error signal*. Here the error signal is the difference between the desired reference level and the output signal *Y* (see Section S1 of the Supporting Information). The ODE for the regulation of *X* by *E* is given by:

$$\frac{dX}{dt} = \alpha_{X,E}E - \beta_X X + b_{S,X} \quad (1)$$

Here,  $\alpha$ ,  $\beta$  and  $b_S$  represent production rate, degradation rate and basal expression level respectively. With *Y* being the output of the process that we want to control, then the ODE describing the regulation of *Y* by *X* and *E* can be written as:

$$\frac{dY}{dt} = \alpha_{Y,X}X + \alpha_{Y,E}E - \beta_Y Y + b_{S,Y} \quad (2)$$

Taking Laplace Transforms of Equations 1 and 2, and after some algebraic manipulation, we obtain the following transfer function (see Section S1 of the Supporting Information):

$$\frac{Y(s)}{E(s)} = \left( \frac{s + \beta_X + (\alpha_{X,E} \alpha_{Y,X} / \alpha_{Y,E})}{s + \beta_X} \right) \left( \frac{\alpha_{Y,E}}{s + \beta_Y} \right) \quad (3)$$

Equation 3 is the open-loop transfer function from  $E$  to  $Y$ . In control theory, an open-loop transfer function is defined as the ratio of the output signal to the input signal in the absence of feedback and it is usually composed of the product of the transfer functions of the controller and the process. In a transfer function, the solutions making the numerator to zero are called the zeros of the system while the solutions making the denominator zero are called the poles of the system. Since  $Y$  is the output of the process, its transfer function is given by  $(\alpha_{Y,E} / (s + \beta_Y))$ . Thus, the transfer function of the controller is then given by  $(s + \beta_X + (\alpha_{X,E} \alpha_{Y,X} / \alpha_{Y,E})) / (s + \beta_X)$ , where the zeros and poles of the controller are  $z = -((\beta_X + (\alpha_{X,E} \alpha_{Y,X} / \alpha_{Y,E})) / \alpha_{Y,E})$  and  $p = -\beta_X$ , respectively. Since  $|p| < |z|$ , we obtain a *phase lag controller*. In control engineering, phase lag controllers are commonly used to improve disturbance rejection and reduce steady-state error,<sup>42</sup> and thus they are well suited to our control objective of achieving perturbation mitigation. Interestingly, based on the schematic diagram of the phase lag controller as shown in Figure 4a, we note that this controller structure is equivalent to a *coherent feedforward loop type-I network motif*,<sup>43, 44</sup> but with an added feedback loop. The role of this network motif in natural biological systems has been subjected to extensive studies and one of its key roles includes perturbation attenuation.<sup>45, 46</sup>

We illustrate here in simulation the use of the genetic phase lag controller in mitigating the perturbation affecting *CHE* in the 9GRN. The configuration for perturbation mitigation using the genetic phase lag controller is shown in Figure 4b. In 9GRN, the output gene  $Y$  is *CHE* and the feedback is delivered by *CHE*'s transcriptional repressor activity on gene  $E$ . As with standard perturbation mitigation strategies in feedback control theory, when a perturbation causes the output level to deviate from its desired level, the controller upon detecting this deviation will react in order to restore the output to its desired level.

As *CHE* is a circadian gene, its expression level is not constant but oscillatory (ATML1 is also light regulated). In the absence of perturbations, the *CHE* expression levels oscillate around the relative expression value of 12.44 (black line in Figure 4c). In our simulations, the perturbation (*B. cinerea* inoculation) is introduced at time 120 hours. Upon infection by *B. cinerea*, the average expression level of *CHE* drops from 12.44 to 9.77 as indicated by the yellow solid line in Figure 4c. The phase lag controller upon detecting this drop in the expression level of *CHE* should exert an appropriate control action to restore the level of *CHE* to its original level. When the phase lag controller is implemented (blue solid line), the controller almost completely attenuates the effect of the perturbation with the level of *CHE* oscillating around 12.33. Moreover, this control strategy is shown to be robust

against variation in model and controller parameters through a Monte Carlo simulation (see Methods section), where we randomly varied the parameters within 20% of their nominal values.

It is known from control theory that to exactly restore the output to the desired reference level after a step disturbance requires an *integral*-type controller.<sup>47</sup> In terms of the controller transfer function, an integral-type controller has a pole at  $s = 0$ . The transfer function of the phase lag controller given in Equation 3 has a pole at  $s = -\beta_x$ , and therefore the slower the degradation rate for  $X$  (which corresponds to a longer mRNA half-life), the more closely the controller will implement an integral-type control action that exactly restores the output to the desired reference level after a disturbance. In Arabidopsis, the longest half-life reported for mRNAs is approximately 26 hours,<sup>40</sup> which corresponds to a degradation rate of 0.026 /hour (calculated using the standard equation for exponential decay,  $\beta = \ln(2)/T$ ) and therefore we have used this value in our simulations (blue solid line in Figure 4c). Full details of all the equations and parameter values underlying the simulations shown in Figure 4c can be found in Section S2.1 of the Supporting Information.

**Controller implementation using regulatory network rewiring.** The direct implementation of the proposed controller in Arabidopsis presents a number of challenges, largely due to the choice of TFs for  $E$  and  $X$  and associated binding sequences. In ref 21, the suggested genes for  $E$  and  $X$  are RhaS ( $E$  in Figure 4a) and XylS ( $X$  in Figure 4a). RhaS activates the production of  $XylS$  and  $CHE$  through a coherent feedforward loop, and XylS also acts as a regulator for the production of  $CHE$ . However, orthogonal TFs may not function in plants whilst using endogenous TFs is likely to have unintended consequences on other processes.

To get around these problems we propose an alternative approach for implementing the proposed controller, based on network rewiring. As shown in Figure 4a, (and Section S6 of the Supporting Information) the structure of a genetic phase lag controller is composed of a coherent feedforward loop type I motif with negative feedback. Thus, if we are able to realize this network motif through the rewiring of the 9GRN, we can obtain a genetic phase lag controller without the need to introduce new non-endogenous genetic circuitry.

For the 9GRN network shown in Figure 2, there are 46 potential rewiring combinations that can realize the network motif of a phase lag controller. However, not all genes within the 9GRN can be used in the rewiring exercise, due to functional constraints. Genes *ATML1*, *LOL1* and *AT1G79150* are not suitable for rewiring, as during *B. cinerea* infection, their expression levels decrease and to use them as part of the positive regulation of the network motif would lead to further decrease in the level of  $CHE$ . Another constraint is due to the gene *at-ERF1*, which is a negative regulator of plant defense (see Figure S1), and hence we would not wish to increase its expression further. Using *at-ERF1* as part of the

positive regulation of the network motif, however, would lead to an increase in its expression. In addition, the gene *ORA59* is a positive regulator of defense, so decreasing its levels would negatively affect the defense response to *B. cinerea*. The gene *RAP2.6L* is highly responsive to stress hormones<sup>30, 48</sup> and while its involvement in infection with *B. cinerea* has not been conclusively proven, we have also chosen to discard rewiring combinations that decrease its levels. Taking these constraints into account, we are left with 11 possible rewiring combinations (see Section S3 of the Supporting Information). Further analysis of these 11 rewiring combinations (see Section S3 of the Supporting Information) reveals that the rewiring strategy that requires the least amount of experimental modification involves the pathway from *MYB51* (*E*) to *ORA59* (*X*) to *CHE* (*Y*). Note that we have included the equivalent function of the genetic phase lag controller in brackets.

Figure 5a shows the rewiring configuration using the pathway from *MYB51* to *ORA59* to *CHE*. To realize the required network motif, *CHE* must inhibit expression of *MYB51*, and *MYB51* and *ORA59* must activate *CHE* expression. Implementing this in simulation, with the perturbation introduced at time 120 hours, we notice only a small recovery in the expression level of *CHE* from around 9.77 to 10.31 after the perturbation (Figure 5a). Why is the increase in the level of *CHE* small given that we have implemented a phase lag controller through network rewiring? From Equation 3, we note that the pole of the phase lag controller is given by the degradation rate of *X*, and in this network motif, this corresponds to the degradation rate of *ORA59*. From Table 3, the value of the degradation rate of *ORA59* is 38.0062, which corresponds to placing the pole at  $s = -38.0062$ . From our previous discussion, it is desirable to have the pole of the controller to be as close to 0 in order for the controller to restore the output to its desired reference level. To move the pole associated with *ORA59* closer to 0, we use positive autoregulation<sup>19, 21, 49</sup>, i.e. we further rewire the network so that *ORA59* activates itself. As expected, with the addition of auto-activation of *ORA59*, we observe that the expression level of *CHE* begins to show a significant increase at around 140 hours. However, instead of returning to its original level, it increases by an extra 15% compared to its original value (Figure 5b). A detailed look at the plot of *MYB51* reveals that the error computed by *MYB51* is higher than expected. The reason for the incorrect error computation is that there is unmodeled regulation affecting *MYB51* (see Equation 4 in Methods section and Section 5 of Supporting Information). As a result, the controller ‘sees’ a larger error than actually exists, and thus exerts a higher control action to mitigate this error, resulting in the observed further increase in the expression level of *CHE*.

To address this issue, a mechanism to negate the effect of unmodeled regulation on *MYB51* is required. This can be achieved by rewiring another gene, for example *ANAC055*, to regulate *MYB51* (see Section S4 in the Supporting Information). As the negation is independent of the process output, this is equivalent to using a feedforward controller. With

the addition of autoregulation and feedforward control, the simulation results in Figure 5c show that the phase lag controller implemented via rewiring is now able to significantly attenuate the effect of the perturbation on *CHE* and return it to its original expression level. Additionally, the Monte Carlo simulations (see Methods section) show that the proposed strategy is robust against parameter variations. The details of the equations and parameter values underlying the simulations shown in Figure 5c can be found in Section S2.2 of the Supporting Information.

**DISCUSSION**

We have presented a novel strategy, based on the use of feedback control, for mitigating the effects of pathogen attack on plant gene regulatory networks, and demonstrated via simulation the ability of this approach to restore the levels of *CHE*, a key defense gene in Arabidopsis, after infection by *B. cinerea*. The use of simple rewiring such as negative autoregulation of *CHE* and direct regulation from ANAC055 was found to be insufficient for restoring the level of *CHE*, therefore we employed a coherent feedforward type I motif with negative feedback. In order to develop the strategy, we employed system identification techniques to build and validate a new dynamical model of the infected gene regulatory sub-network that accurately predicts the type of regulation between each node of the network. Then, using this model, we designed perturbation mitigation strategies using feedback control theory. In the proposed approach, we applied a combination of two positive and one negative regulatory interactions to implement genetic circuitry realizing a phase lag controller. Phase lag controllers are widely used in engineering systems to reduce the effects of disturbances on system performance, and have been proposed as a useful motif for implementing synthetic biological control systems.<sup>21</sup> To date, however, practical strategies for implementing such controllers *in vivo* remain to be elucidated. Here, based on the observation that this control architecture resembles a coherent feedforward loop type-I with negative feedback, we propose a novel controller implementation strategy based on identifying groups of genes within the 9GRN whose regulation can be rewired to realize this network motif. Within the 9GRN, rewiring the pathway from *MYB51* to *ORA59* to *CHE* was shown to provide the most straightforward implementation of the phase lag controller. When suitably augmented with rewired autoregulation and feedforward components, this implementation of the controller was shown to deliver almost perfect perturbation mitigation without the need for any non-endogenous synthetic circuitry.

The regulatory network rewiring described above can be carried out experimentally through the insertion of constructs expressing the desired TF from the appropriate promoter region or TF binding sites combined with a minimal promoter sequence. Given that there are

multiple TF binding sites in a typical promoter sequence (see e.g. ref <sup>50</sup>), it is preferable to use specific TF binding regions. For the rewiring we propose for the 9GRN, regulation of *MYB51* by *CHE*, *CHE* by *ORA59*, and *ORA59* regulation of its own expression, could be achieved using specific promoter regions that have been shown to confer the necessary regulation to drive expression of copies of the target TF coding sequence. *CHE* binds to the promoter of its target gene *CCA1* at the sequence GGTCCCAC.<sup>27</sup> Both the region -363 to -192 bp of the *CCA1* promoter encompassing this sequence and a trimer of the *CHE* binding sequence have been shown to be bound by *CHE*.<sup>27</sup> *ORA59* binds to two GCC boxes (GCCGCC and GCAGCCGCT) in the *PDF1.2* promoter and a tetramer of one of these boxes is sufficient for *ORA59* activation of expression.<sup>51</sup> The other regulatory edges required for rewiring (*MYB51* activation of *CHE* expression and *ANAC055* inhibition of *MYB51*) would currently require using the full length promoter sequences and potentially fusion of transcriptional repression domains. Rewiring using full-length promoter sequences could be achieved relatively quickly (1-2 years) and methods to insert multiple gene constructs into *Arabidopsis* are available (for example, Golden gate cloning<sup>52</sup>). However, the site of insertion of the necessary transgenic constructs (which is not controlled) may also influence resulting levels of expression and hence further optimization/selection of lines with appropriate levels will no doubt be necessary.

The main premise of this paper is to demonstrate potential application of the phase lag controller motif in preventing pathogen-induced perturbations of gene expression. Our 9GRN model is used to demonstrate how a phase lag controller could function. We have provided some evidence for edges in our network, but the presence of additional edges we have not modelled or false positive edges could have a significant impact on the performance of this controller *in vivo*. Strategies such as DAP-seq<sup>29</sup> are making significant improvements in our knowledge of plant TF-promoter interactions but, particularly given the expansion of TF families in plants,<sup>53</sup> greater mapping of plant gene regulatory networks under multiple environmental and developmental conditions will be necessary to drive successful plant synthetic biology strategies. Clearly, in all non-orthogonal rewiring strategies the new edges may have unintended consequences on plant physiology through changing regulatory interactions. In our *in silico* implementation, the controller is only triggered by a significant reduction in *CHE* levels (such as that driven by pathogen infection, not the daily circadian oscillations), and levels of *CHE* and *MYB51* quickly return to normal. The intention of the controller is to maintain oscillating expression levels of *CHE* given its key role in the circadian clock (regulating *CCA1*, a core transcriptional regulator,<sup>27</sup>). We also ensured that expression of positive regulators of defence was not compromised. However, the genes with new rewired links (*MYB51*, *ORA59* and *ANAC055*) are involved in response to other environmental conditions. For example, *MYB51* promotes expression of indolic

glucosinolate biosynthetic genes<sup>54</sup> in response to mechanical stimuli and *ANAC055* is induced by drought, salt and abscisic acid stress.<sup>55</sup> Changes in the expression of these genes due to other stimuli could prevent the controller from operating during *B. cinerea* infection (for example, induction of *ANAC055* would lower levels of MYB51 and indicate a lower level of error to the controller, leading to the controller not reacting properly). Our controller is not designed to handle more than one perturbation (environmentally induced shift in gene expression) and this limitation raises another key challenge in plant systems biology. The development of novel approaches to model and simulate dynamic networks of sufficient size to capture environmental stress cross-talk will significantly improve our ability to rationally engineer stress resilient plants.

**METHODS**

**Transgenic Arabidopsis line.** The CHE T-DNA insertion line, SALK\_143403c, was obtained from the SALK collection<sup>56</sup> and confirmed to be homozygous. Expression of CHE in this line is significantly reduced compared to wildtype (Col-0).<sup>27</sup> The coding region of *at-ERF1* was cloned into the pB7WG2 vector<sup>57</sup> and stable transgenic Arabidopsis lines generated in a Col-4 background. The coding region of *at-ERF1* was cloned into the pB7WG2 vector<sup>57</sup> and stable transgenic Arabidopsis lines generated in a Col-4 background.

**Infection assay.** Arabidopsis plants were grown and *B. cinerea* strain pepper<sup>58</sup> cultured as described in ref 10. Leaves from 5-week-old plants were detached and placed on 0.8% agar in propagator trays. Each leaf was inoculated with a single 10µl droplet of *B. cinerea* inoculum, or a 10µl droplet of sterile grape juice diluted in a 1:1 ratio with sterile water. Each tray contained 9 control leaves and 81 infected leaves, with control and infected leaves in each row. The trays were covered with lids and kept in a growth cabinet under a 16:8 hour light:dark cycle at 22°C, with 90% humidity. Lesion area was assessed from photographs using ImageJ. Mean lesion area of leaves from WT and T-DNA insertion lines were compared using a Student's two-tailed t-test, which assumed equal variance.

**Yeast-1-Hybrid assay.** Yeast-1-Hybrid assays were performed as previously described.<sup>50</sup> Three overlapping promoter regions (of approximately 400 bp) spanning 800 to 1200 bp upstream of the transcription start site were used as bait for transcription factors fused to a GAL4 activation domain in pDEST22 (Invitrogen). Yeast strain AH109 (Clontech) was transformed with these individual TF clones. The promoter fragments were amplified using two-step PCR and cloned into a pDonrZeo vector (Invitrogen) using Gateway cloning. Yeast strain Y187 (Clontech) was transformed with the individual vectors to create the bait strain.

The promoter strain was spotted onto YPDA (yeast, peptone, dextrose, adenine) plates, overlaid with the TF strain, and incubated for 24 hours at 30°C. The diploid cells were replica plated onto selective plates and incubated overnight. This was followed by replica-cleaning and incubation for 4 days, after which growth was scored. Each interaction was tested twice. Primer sequences for the promoter fragments are given in Table 1.

**Table 1: Primer sequences for cloning promoter fragments for Y1H.**

Gene	Forward Primer	Reverse Primer
AT1G06160	AAAAAAGCAGGCTTCGTGCAAT TGATCACTATATTAGTTGAAGT	CAAGAAAGCTGGGTCGTGTCTAA GTGGCACTAAGTTTGGG
AT1G06160	AAAAAAGCAGGCTTCCCGCCTT AGTTTCTGACAGAGTTTCGACTC	CAAGAAAGCTGGGTCGAGTGTA TGACGTACGGCGGCGTATTCCCG
AT1G06160	AAAAAAGCAGGCTTCCTGTTCTG TCGAGTTGTTGCTTGTTGAGCC	CAAGAAAGCTGGGTCGTGTGGGCA AAATAGGTCAAACATGCGGC
AT3G15500	GGGGGAATTCATAAGAGGAGGT ACAGTCACACA	GGGGAAGCTTACGCGTCGAAG CTCTGCTACTCGTGTATGTAT
AT3G15500	GGCCGAATTCATCCCATCATTC ACTTACAC	GGGGAAGCTTACGCGTGATCAA TTAGAGCGTCGTGATTTATGC
AT3G15500	GGGGGAATTCGTTTGTGTTTGT TCCCTCTCTCTGA	GGGGAAGCTTACGCGTTGAGTT ACATAACAGTGACAATCTACGA
AT3G15500	GGGGGAATTCGAGAAGCGTGT TTGTGTTATACGGACTTA	GGGGAAGCTTACGCGTTGTGTC TATTGGTTGAGTTAGGC

**Accession numbers.** Arabidopsis gene names and AGI locus codes referred to in this article are shown in Table 2.

**Table 2: Associated AGI to Arabidopsis gene names.**

Gene name	AGI
<i>ORA59</i>	AT1G06160
<i>MYB51</i>	AT1G18570
<i>LOL1</i>	AT1G32540
<i>AT1G79150</i>	AT1G79150
<i>ANAC055</i>	AT3G15500
<i>at-ERF1</i>	AT4G17500
<i>ATML1</i>	AT4G21750
<i>CHE</i>	AT5G08330
<i>RAP2.6L</i>	AT5G13330

**Generating the TF network.** An Arabidopsis TF list was generated by combining lists from ThaleMine<sup>59</sup>, DATF<sup>60</sup>, ref<sup>61</sup>, and homology searches using DNA binding domains, followed by manual curation of genes only identified in one list. The final list of 2,534 genes is given in Supplementary File 1b. The list of Arabidopsis genes differentially expressed during *B. cinerea* infection was obtained from ref 10, which included 883 differentially expressed TFs (Supplementary File 1a).



**Generating a dynamic model of the CHE regulatory sub-network.** Traditionally, a model of a gene regulatory network comprises both transcription and translation mechanisms. However, in our case, given that only mRNA accumulation time-series data are available<sup>10</sup>, the following two assumptions are made in building the 9GRN model. Firstly, the translation of the protein from mRNA follows a linear relationship and secondly, the behavior of the translated protein follows its mRNA closely. With these two assumptions, we can group together the protein translation rate with the mRNA transcription rate resulting in the entire 9GRN being modeled using only mRNA data. Based on the above assumptions, the model of the 9GRN shown in Figure 2 can be described by the following ODEs:

$$\begin{aligned}
 \frac{dN_{ORA}}{dt} &= \alpha_{ORA,1}N_{MYB} + \alpha_{ORA,2}N_{ANA} + \alpha_{ORA,3}N_{ERF} + \beta_{ORA}N_{ORA} + b_{S,ORA} \\
 \frac{dN_{MYB}}{dt} &= \beta_{MYB}N_{MYB} + b_{S,MYB} + c_{MYB}W \\
 \frac{dN_{LOL}}{dt} &= \beta_{LOL}N_{LOL} + b_{S,LOL} + c_{LOL}W \\
 \frac{dN_{AT1}}{dt} &= \alpha_{AT1,1}N_{CHE} + \alpha_{AT1,2}N_{RAP} + \beta_{AT1}N_{AT1} + b_{S,AT1} + c_{AT1}W \\
 \frac{dN_{ANA}}{dt} &= \alpha_{ANA,1}N_{RAP} + \beta_{ANA}N_{ANA} + b_{S,ANA} + c_{ANA}W \\
 \frac{dN_{ERF}}{dt} &= \beta_{ERF}N_{ERF} + b_{S,ERF} + c_{ERF}W \\
 \frac{dN_{ATM}}{dt} &= \alpha_{ATM,1}N_{RAP} + \beta_{ATM}N_{ATM} + b_{S,ATM} + c_{ATM}W + \gamma_{ATM}L \\
 \frac{dN_{CHE}}{dt} &= \alpha_{CHE,1}N_{LOL} + \alpha_{CHE,2}N_{AT1} + \alpha_{CHE,3}N_{ATM} + \beta_{CHE}N_{CHE} + b_{S,CHE} + \gamma_{CHE}L \\
 \frac{dN_{RAP}}{dt} &= \alpha_{RAP,1}N_{ANA} + \beta_{RAP}N_{RAP} + b_{S,RAP} + c_{RAP}W
 \end{aligned} \tag{4}$$

where  $\alpha_{ij} \in (-\infty, +\infty)$ ,  $\beta_i > 0$ ,  $\gamma_{CHE} > 0$ ,  $b_{S,i} \in (-\infty, +\infty)$ , and  $c_i \in (-\infty, +\infty)$  are the unknown parameters that represent the production rate, degradation rate, scaled light effect, basal level and effect of the unmodeled regulation, respectively, with  $i$  and  $j$  denoting the appropriate indices describing the parameters given in Equation 4.  $N_i$  represents the gene.  $W$  represents the effect of the unmodeled regulation (e.g. direct regulation as a result of *B. cinerea* infection, noise and other regulations not identified by the network inference algorithms), where  $W = 0$  (resp.  $W = 1$ ) is used when the effect is absent (respectively present). In the experiments from which our data were generated<sup>10</sup>, the time-series data from the control and infected experiments are treated as a continuous dataset where the infection starts at the halfway point, i.e., time 48 hours. Thus, the transition of  $W$  from 0 to 1 is not modeled as an instantaneous change but as a gradual increase.  $L$  represents the

effect of light and *CHE* follows a sinusoidal rhythm as known.<sup>27</sup> For details on the mathematical representation for *W* and *L* see Section S5 of the Supporting Information.

The values of the model parameters were estimated from the available mRNA time-series data using a nonlinear least squares algorithm and the estimated parameters are given in Table 3.

**Table 3: Estimated parameters of the linear model**

Gene Name	Values
<i>ORA59</i>	$\alpha_{ORA,1} = 14.3800$ , $\alpha_{ORA,2} = -0.7359$ , $\alpha_{ORA,3} = 21.5714$ , $\beta_{ORA} = -38.0062$ , $b_{S,ORA} = 15.2355$
<i>MYB51</i>	$\beta_{MYB} = -0.6658$ , $b_{MYB} = 5.6277$ , $c_{MYB} = 1.1890$
<i>LOL1</i>	$\beta_{LOL} = -0.0485$ , $b_{S,LOL} = 0.4874$ , $c_{LOL} = -0.1241$
<i>AT1G79150</i>	$\alpha_{AT1,1} = 0.7577$ , $\alpha_{AT1,2} = -0.7408$ , $\beta_{AT1} = -2.4088$ , $b_{S,AT1} = 23.863$ , $c_{AT1} = 0.91809$
<i>ANAC055</i>	$\alpha_{ANA,1} = 25.6935$ , $\beta_{ANA} = -28.4685$ , $b_{S,ANA} = 0.0517$ , $c_{ANA} = 82.5415$
<i>at-ERF1</i>	$\beta_{ERF} = -0.2051$ , $b_{S,ERF} = 1.8699$ , $c_{ERF} = 0.8735$
<i>ATML1</i>	$\alpha_{ATM,1} = -0.7945$ , $\beta_{ATM} = -1.1142$ , $b_{S,ATM} = 19.3684$ , $c_{ATM} = 0.0040$ , $\gamma_{ATM} = 0.5000$
<i>CHE</i>	$\alpha_{CHE,1} = 24.5024$ , $\alpha_{CHE,2} = 3.3801$ , $\alpha_{CHE,3} = 17.6771$ , $\beta_{CHE} = -40.1258$ , $b_{S,CHE} = 3.7167$ , $\gamma_{CHE} = 16.8001$
<i>RAP2.6L</i>	$\alpha_{RAP,1} = 0.4186$ , $\beta_{RAP} = -0.7933$ , $b_{S,RAP} = 3.7046$ , $c_{RAP} = 0.0045$

All the simulations of the ODE models, phase genetic controller and network rewiring are done using MATLAB built-in solver *ode45*, and the initial condition for each gene to solve the ODE is the first data point of the mRNA time-series for each respective gene. For the simulation using the genetic phase lag controller (Equation S2.1), the initial conditions for solving the ODEs for *X* and *E* are set to 0.

**Parameter estimation.** For the 9GRN linear model, the values of the unknown parameters are estimated from the available mRNA time-series using nonlinear least square, given by

$$\hat{\theta} = \arg \min_{\theta} \frac{1}{N_L} \sum_{i \in \psi} \sum_{t=1}^{N_L} [N_i(t) - \hat{N}_i(t, \theta)]^2 \quad (5)$$

where  $\theta = [\alpha_i, \beta_i, b_{S,i}, c_i]$  with  $i \in \psi = [ORA, MYB, LOL, AT1, ANA, ERF, ATM, CHE, RAP]$ ,

$N_L$  is the length of the time-series data,  $\hat{N}$  is the simulated data from Equation 4 and  $N$  is the experimental data, which are the mRNA time-series taken from ref 10. There are four sets of mRNA time-series and we use the average mRNA expression from the first three sets for parameter estimation and use the fourth data set as an independent data set for validating the ODE model. Equation 5 is solved using MATLAB function *fminsearch* which uses the Nelder-Mead simplex algorithm.

As a quantitative measure of the model performance, we compute the Mean Square Error (MSE) for each gene between the experimental data and the model given by Equation 4. The MSE for each gene is computed as follows:

$$\text{MSE} = \frac{1}{N_L} \sum_{t=1}^{N_L} [N(t) - \hat{N}(t, \theta)]^2 \tag{6}$$

The total MSE,  $\text{MSE}_T$  is computed by summing the MSE for all nine genes in the 9GRN. Table 4 shows the MSE values for both the training and validation data sets.

Table 4: MSE for both training and validation data sets.

Gene Name	MSE (Training)	MSE (Validation)
<i>ORA59</i>	0.7730	1.9828
<i>MYB51</i>	0.3910	0.6949
<i>LOL1</i>	0.3703	0.6582
<i>AT1G79150</i>	0.1829	0.3587
<i>ANAC055</i>	0.9889	2.3849
<i>at-ERF1</i>	0.4394	1.0583
<i>ATML1</i>	0.3746	0.6682
<i>CHE</i>	0.8759	1.0819
<i>RAP2.6L</i>	0.3452	0.6366
$\text{MSE}_T$	4.7410	9.5245

**Performance and robustness analysis.** To analyze the performance and robustness of the proposed strategies, we perform a Monte Carlo simulation where we randomly draw all the parameters from a uniform distribution. Then, we vary the parameters within ranges of 20%, around their nominal values. Mathematically, we have  $p(1 + \Delta P(x))$ , where  $p$  denotes the model and the controller parameters,  $P(x)$  is the probability distribution and  $\Delta = 0.2$ . Using the Chernoff bound and associated guidelines for Monte Carlo simulation, a total number of 1060 simulations is required to achieve an accuracy level of 0.05 with a confidence level of 99%.<sup>62, 63</sup>

ASSOCIATED CONTENT

Supporting Information

Comprises supplementary text, supplementary figures and supplementary files referenced in this article. The supplementary files contain lists of Arabidopsis TF genes, their associated biological functions and TF genes that are differentially expressed during *B. cinerea* infection. These are available free of charge via the Internet at <http://pubs.acs.org>

AUTHOR INFORMATION

Corresponding Authors

Email: d.bates@warwick.ac.uk, katherine.denby@york.ac.uk

## Author Contributions

KJD and DGB conceived the study. MF and IG developed the models and simulations. Experimental data was generated by by PZ and IG. MF, IG, DGB, and KJD analyzed the data. All authors reviewed and wrote the manuscript. <sup>†</sup>MF and IG are joint first authors. MF is currently with the School of Mechanical, Aerospace and Automotive Engineering, Coventry University, CV1 5FB, United Kingdom.

## Notes

The authors declare no competing financial interests.

## ACKNOWLEDGEMENTS

This work was supported by the Biotechnological and Biological Sciences Research Council (BBSRC)/Engineering and Physical Sciences Research Council (EPSRC) Warwick Integrative Synthetic Biology Centre (WISB) via research grant BB/M017982/1 (MF, KJD, DGB) and the EPSRC/BBSRC Oxford/Warwick/Bristol Centre for Doctoral Training in Synthetic Biology (SynBio CDT) via research grant EP/L016494/1 (IG). PZ and KJD were supported by the BBRSC/EPSRC-funded grant Plant Response to Environmental Stress *Arabidopsis* (BB/F005806/1).

## REFERENCES

- (1) Bebber, D. P.; Ramotowski, M. A. T.; Gurr, S. J. (2013) Crop pests and pathogens move polewards in a warming world. *Nature Clim. Change* 3, 985-988.
- (2) Bebber, D. P.; Holmes, T.; Gurr, S. J. (2014) The global spread of crop pests and pathogens. *Glob. Ecol. Biogeogr.* 23, 1398-1407.
- (3) Buchanan-Wollaston, V.; Wilson, Z.; Tardieu, F.; Beynon, J.; Denby, K. (2017) Harnessing diversity from ecosystems to crops to genes. *Food Energy Secur.* 6, 19-25.
- (4) Parmar, N.; Singh, K. H.; Sharma, D.; Singh, L.; Kumar, P.; Nanjundan, J.; Khan, Y. J.; Chauhan, D. K.; Thakur, A. K. (2017) Genetic engineering strategies for biotic and abiotic stress tolerance and quality enhancement in horticultural crops: a comprehensive review. 3 *Biotech* 7, 239.
- (5) Veronese, P.; Nakagami, H.; Bluhm, B.; AbuQamar, S.; Chen, X.; Salmeron, J.; Dietrich, R. A.; Hirt, H.; Mengiste, T. (2006) The membrane-anchored BOTRYTIS-INDUCED KINASE1 plays distinct roles in *Arabidopsis* resistance to necrotrophic and biotrophic pathogens. *Plant Cell* 18, 257-273.
- (6) Wilkins, O.; Hafemeister, C.; Plessis, A.; Holloway-Phillips, M.-M.; Pham, G. M.; Nicotra, A. B.; Gregorio, G. B.; Jagadish, S. V. K.; Septiningsih, E. M.; Bonneau, R.; Purugganan, M. (2016) EGRINs (Environmental Gene Regulatory Influence Networks) in rice that function in

the response to water deficit, high temperature, and agricultural environments. *Plant Cell* 28, 2365-2384.

(7) Lewis, L. A.; Polanski, K.; de Torres-Zabala, M.; Jayaraman, S.; Bowden, L.; Moore, J.; Penfold, C. A.; Jenkins, D. J.; Hill, C.; Baxter, L.; Kulasekaran, S.; Truman, W.; Littlejohn, G.; Prusinska, J.; Mead, A.; Steinbrenner, J.; Hickman, R.; Rand, D.; Wild, D. L.; Ott, S.; Buchanan-Wollaston, V.; Smirnov, N.; Beynon, J.; Denby, K.; Grant, M. (2015) Transcriptional dynamics driving MAMP-triggered immunity and pathogen effector-mediated immunosuppression in *Arabidopsis* leaves following infection with *Pseudomonas syringae* pv tomato DC3000. *Plant Cell* 27, 3038-3064.

(8) Breeze, E.; Harrison, E.; McHattie, S.; Hughes, L.; Hickman, R.; Hill, C.; Kiddle, S.; Kim, Y.-s.; Penfold, C. A.; Jenkins, D.; Zhang, C.; Morris, K.; Jenner, C.; Jackson, S.; Thomas, B.; Tabrett, A.; Legaie, R.; Moore, J. D.; Wild, D. L.; Ott, S.; Rand, D.; Beynon, J.; Denby, K.; Mead, A.; Buchanan-Wollaston, V. (2011) High-resolution temporal profiling of transcripts during *Arabidopsis* leaf senescence reveals a distinct chronology of processes and regulation. *Plant Cell* 23, 873-894.

(9) Sharma, R.; De Vleeschauwer, D.; Sharma, M. K.; Ronald, P. C. (2013) Recent advances in dissecting stress-regulatory crosstalk in rice. *Mol. Plant* 6, 250-260.

(10) Windram, O.; Madhou, P.; McHattie, S.; Hill, C.; Hickman, R.; Cooke, E.; Jenkins, D. J.; Penfold, C. A.; Baxter, L.; Breeze, E.; Kiddle, S. J.; Rhodes, J.; Atwell, S.; Kliebenstein, D. J.; Kim, Y.-s.; Stegle, O.; Borgwardt, K.; Zhang, C.; Tabrett, A.; Legaie, R.; Moore, J.; Finkenstadt, B.; Wild, D. L.; Mead, A.; Rand, D.; Beynon, J.; Ott, S.; Buchanan-Wollaston, V.; Denby, K. J. (2012) *Arabidopsis* defense against *Botrytis cinerea*: chronology and regulation deciphered by high-resolution temporal transcriptomic analysis. *Plant Cell* 24, 3530-3557.

(11) Williamson, B.; Tudzynski, B.; Tudzynski, P.; Van Kan, J. A. L. (2007) *Botrytis cinerea*: the cause of grey mould disease. *Mol. Plant Pathol.* 8, 561-580.

(12) Jamir, Y.; Guo, M.; Oh, H.-S.; Petnicki-Ocwieja, T.; Chen, S.; Tang, X.; Dickman, M. B.; Collmer, A.; R. Alfano, J. (2004) Identification of *Pseudomonas syringae* type III effectors that can suppress programmed cell death in plants and yeast. *Plant J.* 37, 554-565.

(13) Weiberg, A.; Wang, M.; Lin, F.-M.; Zhao, H.; Zhang, Z.; Kaloshian, I.; Huang, H.-D.; Jin, H. (2013) Fungal small RNAs suppress plant immunity by hijacking host RNA interference pathways. *Science* 342, 118-123.

(14) Jones, J. D. G.; Dangl, J. L. (2006) The plant immune system. *Nature* 444, 323-329.

(15) Heidel, A. J.; Clarke, J. D.; Antonovics, J.; Dong, X. (2004) Fitness costs of mutations affecting the systemic acquired resistance pathway in *Arabidopsis thaliana*. *Genetics* 168, 2197-2206.

(16) Hespanha, J. P.; Naghshtabrizi, P.; Xu, Y. (2007) A survey of recent results in networked control systems. *Proc. IEEE* 95, 138-162.

(17) Liu, Y.-Y.; Slotine, J.-J.; Barabasi, A.-L. (2011) Controllability of complex networks. *Nature* 473, 167-173.

(18) Vinayagam, A.; Gibson, T. E.; Lee, H.-J.; Yilmazel, B.; Roesel, C.; Hu, Y.; Kwon, Y.; Sharma, A.; Liu, Y.-Y.; Perrimon, N.; Barabási, A.-L. (2016) Controllability analysis of the

directed human protein interaction network identifies disease genes and drug targets. *Proc. Natl. Acad. Sci. USA* 113, 4976-4981.

(19) Ang, J.; Bagh, S.; Ingalls, B. P.; McMillen, D. R. (2010) Considerations for using integral feedback control to construct a perfectly adapting synthetic gene network. *J. Theor. Biol.* 266, 723-738.

(20) Briat, C.; Zechner, C.; Khammash, M. (2016) Design of a synthetic integral feedback circuit: dynamic analysis and DNA implementation. *ACS Synth. Biol.* 5, 1108-1116.

(21) Harris, A. W. K.; Dolan, J. A.; Kelly, C. L.; Anderson, J.; Papachristodoulou, A. (2015) Designing genetic feedback controllers. *IEEE Trans. Biomed. Circuits Syst.* 9, 475-484.

(22) Huynh-Thu, V. A.; Irrthum, A.; Wehenkel, L.; Geurts, P. (2010) Inferring regulatory networks from expression data using tree-based methods. *PLoS ONE* 5, e12776.

(23) Haury, A.-C.; Mordellet, F.; Vera-Licona, P.; Vert, J.-P. (2012) TIGRESS: trustful inference of gene regulation using stability selection. *BMC Syst. Biol.* 6.

(24) Bonneau, R.; Reiss, D. J.; Shannon, P.; Facciotti, M.; Hood, L.; Baliga, N. S.; Thorsson, V. (2006) The inferelator: an algorithm for learning parsimonious regulatory networks from systems-biology data sets *de novo*. *Genome Biol.* 7, R36.

(25) Schaffter, T.; Marbach, D.; Floreano, D. (2011) GeneNetWeaver: in silico benchmark generation and performance profiling of network inference methods. *Bioinformatics* 27, 2263-2270.

(26) Marbach, D.; Costello, J. C.; Kuffner, R.; Vega, N. M.; Prill, R. J.; Camacho, D. M.; Allison, K. R.; Kellis, M.; Collins, J. J.; Stolovitzky, G. (2012) Wisdom of crowds for robust gene network inference. *Nat. Meth.* 9, 796-804.

(27) Pruneda-Paz, J. L.; Breton, G.; Para, A.; Kay, S. A. (2009) A functional genomics approach reveals CHE as a component of the *Arabidopsis* circadian clock. *Science* 323, 1481-1485.

(28) Pré, M.; Atallah, M.; Champion, A.; De Vos, M.; Pieterse, C. M. J.; Memelink, J. (2008) The AP2/ERF domain transcription factor ORA59 integrates jasmonic acid and ethylene signals in plant defense. *Plant Physiol.* 147, 1347-1357.

(29) O'Malley, Ronan C.; Huang, S.-shan C.; Song, L.; Lewsey, Mathew G.; Bartlett, A.; Nery, Joseph R.; Galli, M.; Gallavotti, A.; Ecker, Joseph R. (2016) Cistrome and epicistrome features shape the regulatory DNA landscape. *Cell* 165, 1280-1292.

(30) Hickman, R.; van Verk, M. C.; Van Dijken, A. J. H.; Pereira Mendes, M.; Vroegop-Vos, I. A.; Caarls, L.; Steenbergen, M.; Van Der Nagel, I.; Wesselink, G. J.; Jironkin, A.; Talbot, A.; Rhodes, J.; de Vries, M.; Schuurink, R. C.; Denby, K.; Pieterse, C. M. J.; Van Wees, S. C. M. (2017) Architecture and dynamics of the jasmonic acid gene regulatory network. *Plant Cell*, Aug, 2017. DOI:10.1105/tpc.16.00958.

(31) Gardner, T. S.; di Bernardo, D.; Lorenz, D.; Collins, J. J. (2003) Inferring genetic networks and identifying compound mode of action via expression profiling. *Science* 301, 102-105.

- (32) di Bernardo, D.; Thompson, M. J.; Gardner, T. S.; Chobot, S. E.; Eastwood, E. L.; Wojtovich, A. P.; Elliott, S. J.; Schaus, S. E.; Collins, J. J. (2005) Chemogenomic profiling on a genome-wide scale using reverse-engineered gene networks. *Nat. Biotech.* 23, 377-383.
- (33) Bansal, M.; Belcastro, V.; Ambesi-Impiombato, A.; di Bernardo, D. (2007) How to infer gene networks from expression profiles. *Mol. Syst. Biol.* 3.
- (34) Dalchau, N.; Baek, S. J.; Briggs, H. M.; Robertson, F. C.; Dodd, A. N.; Gardner, M. J.; Stancombe, M. A.; Haydon, M. J.; Stan, G.-B.; Gonçalves, J. M.; Webb, A. A. R. (2011) The circadian oscillator gene GIGANTEA mediates a long-term response of the *Arabidopsis thaliana* circadian clock to sucrose. *Proc. Natl. Acad. Sci. USA* 108, 5104-5109.
- (35) Herrero, E.; Kolmos, E.; Bujdoso, N.; Yuan, Y.; Wang, M.; Berns, M. C.; Uhlworm, H.; Coupland, G.; Saini, R.; Jaskolski, M.; Webb, A.; Gonçalves, J.; Davis, S. J. (2012) EARLY FLOWERING4 recruitment of EARLY FLOWERING3 in the nucleus sustains the *Arabidopsis* circadian clock. *Plant Cell* 24, 428-443.
- (36) Kim, J.; Bates, D. G.; Postlethwaite, I.; Heslop-Harrison, P.; Cho, K.-H. (2007) Least-squares methods for identifying biochemical regulatory networks from noisy measurements. *BMC Bioinform.* 8, 8.
- (37) Kim, J.; Bates, D. G.; Postlethwaite, I.; Heslop-Harrison, P.; Cho, K.-H. (2008) Linear time-varying models can reveal non-linear interactions of biomolecular regulatory networks using multiple time-series data. *Bioinformatics* 24, 1286-1292.
- (38) Wu, H.; Kerr, M.; Cui, X.; Churchill, G. (2003) MAANOVA: a software package for the analysis of spotted cDNA microarray experiments. *The Analysis of Gene Expression Data*, 313-341.
- (39) Yang, Y. H.; Dudoit, S.; Luu, P.; Lin, D. M.; Peng, V.; Ngai, J.; Speed, T. P. (2002) Normalization for cDNA microarray data: a robust composite method addressing single and multiple slide systematic variation. *Nucleic Acids Res.* 30, e15.
- (40) Narsai, R.; Howell, K. A.; Millar, A. H.; O'Toole, N.; Small, I.; Whelan, J. (2007) Genome-wide analysis of mRNA decay rates and their determinants in *Arabidopsis thaliana*. *Plant Cell* 19, 3418-3436.
- (41) Ang, J.; McMillen, David R. (2013) Physical constraints on biological integral control design for homeostasis and sensory adaptation. *Biophys. J.* 104, 505-515.
- (42) Franklin, G. F.; Powell, J. D.; Emami-Naeini, A. (2015) *Feedback control of dynamic systems*. 7th ed.; Pearson.
- (43) Milo, R.; Shen-Orr, S.; Itzkovitz, S.; Kashtan, N.; Chklovskii, D.; Alon, U. (2002) Network motifs: simple building blocks of complex networks. *Science* 298, 824-827.
- (44) Alon, U. (2007) Network motifs: theory and experimental approaches. *Nat. Rev. Genet.* 8, 450-461.
- (45) Ma, W.; Trusina, A.; El-Samad, H.; Lim, W. A.; Tang, C. (2009) Defining network topologies that can achieve biochemical adaptation. *Cell* 138, 760-773.
- (46) Huang, X. N.; Ren, H. P. (2017) Understanding robust adaptation dynamics of gene regulatory network. *IEEE Trans. Biomed. Circuits Syst.* 11, 942-957.

- (47) Ogata, K. (2009) *Modern control engineering*. 5th ed.; Pearson.
- (48) Krishnaswamy, S.; Verma, S.; Rahman, M. H.; Kav, N. N. V. (2011) Functional characterization of four APETALA2-family genes (RAP2.6, RAP2.6L, DREB19 and DREB26) in *Arabidopsis*. *Plant Mol. Biol.* 75, 107-127.
- (49) Drengstig, T.; Ni, X. Y.; Thorsen, K.; Jolma, I. W.; Ruoff, P. (2012) Robust adaptation and homeostasis by autocatalysis. *J. Phys. Chem. B* 116, 5355-5363.
- (50) Hickman, R.; Hill, C.; Penfold, C. A.; Breeze, E.; Bowden, L.; Moore, J. D.; Zhang, P.; Jackson, A.; Cooke, E.; Bewicke-Copley, F.; Mead, A.; Beynon, J.; Wild, D. L.; Denby, K. J.; Ott, S.; Buchanan-Wollaston, V. (2013) A local regulatory network around three NAC transcription factors in stress responses and senescence in *Arabidopsis* leaves. *Plant J.* 75, 26-39.
- (51) Zarei, A.; Körbes, A. P.; Younessi, P.; Montiel, G.; Champion, A.; Memelink, J. (2011) Two GCC boxes and AP2/ERF-domain transcription factor ORA59 in jasmonate/ethylene-mediated activation of the PDF1.2 promoter in *Arabidopsis*. *Plant Mol. Biol.* 75, 321-331.
- (52) Engler, C.; Gruetzner, R.; Kandzia, R.; Marillonnet, S. (2009) Golden gate shuffling: a one-pot DNA shuffling method based on type IIs restriction enzymes. *PLoS ONE* 4, e5553.
- (53) Shiu, S.-H.; Shih, M.-C.; Li, W.-H. (2005) Transcription factor families have much higher expansion rates in plants than in animals. *Plant Physiol.* 139, 18-26.
- (54) Gigolashvili, T.; Berger, B.; Mock, H.-P.; Müller, C.; Weisshaar, B.; Flügge, U.-I. (2007) The transcription factor HIG1/MYB51 regulates indolic glucosinolate biosynthesis in *Arabidopsis thaliana*. *Plant J.* 50, 886-901.
- (55) Tran, L.-S. P.; Nakashima, K.; Sakuma, Y.; Simpson, S. D.; Fujita, Y.; Maruyama, K.; Fujita, M.; Seki, M.; Shinozaki, K.; Yamaguchi-Shinozaki, K. (2004) Isolation and functional analysis of *Arabidopsis* stress-inducible NAC transcription factors that bind to a drought-responsive *cis*-element in the *early responsive to dehydration stress 1* promoter. *Plant Cell* 16, 2481-2498.
- (56) Alonso, J. M.; Stepanova, A. N.; Leisse, T. J.; Kim, C. J.; Chen, H.; Shinn, P.; Stevenson, D. K.; Zimmerman, J.; Barajas, P.; Cheuk, R.; Gadrinab, C.; Heller, C.; Jeske, A.; Koesema, E.; Meyers, C. C.; Parker, H.; Prednis, L.; Ansari, Y.; Choy, N.; Deen, H.; Geralt, M.; Hazari, N.; Hom, E.; Karnes, M.; Mulholland, C.; Ndubaku, R.; Schmidt, I.; Guzman, P.; Aguilar-Henonin, L.; Schmid, M.; Weigel, D.; Carter, D. E.; Marchand, T.; Risseuw, E.; Brogden, D.; Zeko, A.; Crosby, W. L.; Berry, C. C.; Ecker, J. R. (2003) Genome-wide insertional mutagenesis of *Arabidopsis thaliana*. *Science* 301, 653-657.
- (57) Karimi, M.; Inzé, D.; Depicker, A. (2002) GATEWAY™ vectors for *Agrobacterium*-mediated plant transformation. *Trends Plant Sci.* 7, 193-195.
- (58) Denby, K. J.; Kumar, P.; Kliebenstein, D. J. (2004) Identification of *Botrytis cinerea* susceptibility loci in *Arabidopsis thaliana*. *Plant J.* 38, 473-486.
- (59) Krishnakumar, V.; Hanlon, M. R.; Contrino, S.; Ferlanti, E. S.; Karamycheva, S.; Kim, M.; Rosen, B. D.; Cheng, C.-Y.; Moreira, W.; Mock, S. A.; Stubbs, J.; Sullivan, J. M.; Krampis, K.; Miller, J. R.; Micklem, G.; Vaughn, M.; Town, C. D. (2015) Araport: the *Arabidopsis* information portal. *Nucleic Acids Res.* 43, D1003-D1009.



(60) Guo, A.; He, K.; Liu, D.; Bai, S.; Gu, X.; Wei, L.; Luo, J. (2005) DATF: a database of Arabidopsis transcription factors. *Bioinformatics* 21, 2568-2569.

(61) Pruneda-Paz, Jose L.; Breton, G.; Nagel, Dawn H.; Kang, S. E.; Bonaldi, K.; Doherty, Colleen J.; Ravelo, S.; Galli, M.; Ecker, Joseph R.; Kay, Steve A. (2014) A genome-scale resource for the functional characterization of *Arabidopsis* transcription factors. *Cell Rep.* 8, 622-632.

(62) Vidyasagar, M. (1998) Statistical learning theory and randomized algorithms for control. *IEEE Control Syst.* 18, 69-85.

(63) Menon, P. P.; Postlethwaite, I.; Bennani, S.; Marcos, A.; Bates, D. G. (2009) Robustness analysis of a reusable launch vehicle flight control law. *Control Eng. Pract.* 17, 751-765.

**Figure 1.** Expression and role of CHE during infection with *B. cinerea*. (a) Expression of the TF CHE is downregulated during *B. cinerea* infection of Arabidopsis leaves. Leaves were drop-inoculated with *B. cinerea* spores or mock-inoculated, and genome-wide gene expression determined every 2 hours for both mock treatment (blue) and *B. cinerea* infection (red). Open circles are the average of four biological repeats with bars representing standard deviation. This data is extracted from Windram et al.<sup>10</sup>. (b) CHE is a positive regulator of defence against *B. cinerea*. Lesion size of Arabidopsis leaves ( $n = 17$ ) drop-inoculated with *B. cinerea* spores were measured 36 and 72 hours post infection. *che-1* is an Arabidopsis mutant with significantly reduced CHE expression. WT is the wildtype Col-0 Arabidopsis accession. Error bars represent standard deviation, \*\* represents  $p \leq 0.01$  and \*\*\* represents  $p \leq 0.001$ .

**Figure 2.** Network model of gene regulatory events mediating transcriptional response to *Botrytis cinerea*. The nine-gene network (9GRN) is a sub-network of the initial network model inferred from time series transcriptome data. The direction of regulation is indicated by the arrow. Red stars represent unmodeled regulation (e.g. direct regulation from *B. cinerea*, noise and other unidentified regulation, see also Section S5 of the Supporting Information). The yellow circle represents circadian regulation. Green edges represent interactions that are supported by experimental data. The regulation types (arrow-head and bar-head) in 9GRN are identified through system identification.

**Figure 3.** Validation of the linear model against an experimental data set that was not used in the parameter estimation exercise. The experimental data sets in ref 10 are composed of two time series, one mock-inoculated and one *B. cinerea*-inoculated. Here, these two time series are joined (denoted by the vertical dashed line) to illustrate a transition from pre- to

post-infection, with *B. cinerea* infection starting at time 48 hours. There are four sets of such joined time-series data; we used the average of the first three data sets for parameter estimation (see Figure S3), leaving the fourth data set for model validation shown above. We have also included the unmodeled regulation,  $W$  described by Equation S5.1. Line with dots: Experiment data, Solid line: Linear model.

**Figure 4.** Perturbation mitigation using a genetic phase lag controller. (a) Genetic circuit of the proposed controller.  $X$  is the output of the controller,  $Y$  is the output of the process and  $E$  computes the error signal. This genetic circuit is equivalent to a coherent feedforward loop type-I with feedback network motif that yields the transfer function of a phase lag controller plus process dynamics. (b) Implementation of the phase lag controller motif for perturbation mitigation in the 9GRN. (c) Simulation results of phase lag controller in mitigating perturbation in the 9GRN. The solid black line is the desired average expression of *CHE*, the solid yellow line is the expression of *CHE* during infection with *B. cinerea* without any control action, and the solid blue lines represent gene expression during infection with *B. cinerea* with control action. The gray shaded regions represent the expression level with uncertainty obtained through Monte Carlo simulation. In our simulations, the parameter values for the phase lag controller are  $\alpha_{X,E} = 3.00$ ,  $\alpha_{Y,X} = 5.00$ ,  $\alpha_{Y,E} = 5.00$ ,  $\beta_X = 0.026$ , while the parameter values for the error computation are  $b_{S,E} = 6.21$  and  $\gamma = \beta_E = 0.50$ . For more details on the choice of these values, see Figures S6 to S8.

**Figure 5.** Simulation results for genes in the 9GRN with proposed network rewiring. Black line: reference value, Blue line: gene expression level in response to *B. cinerea* infection after rewiring. Yellow line: gene expression level in response to *B. cinerea* infection without network rewiring. Perturbation (inoculation) is given at time 120 hours. (a) Rewiring a controller by adding activation of *CHE* by MYB51 and ORA59 and inhibition of MYB51 expression by CHE. (b) Addition of positive autoregulation to ORA59. (c) Addition of feedforward component; inhibition of MYB51 by ANAC055. The gray shaded regions represent the expression level with uncertainty obtained through Monte Carlo simulation.

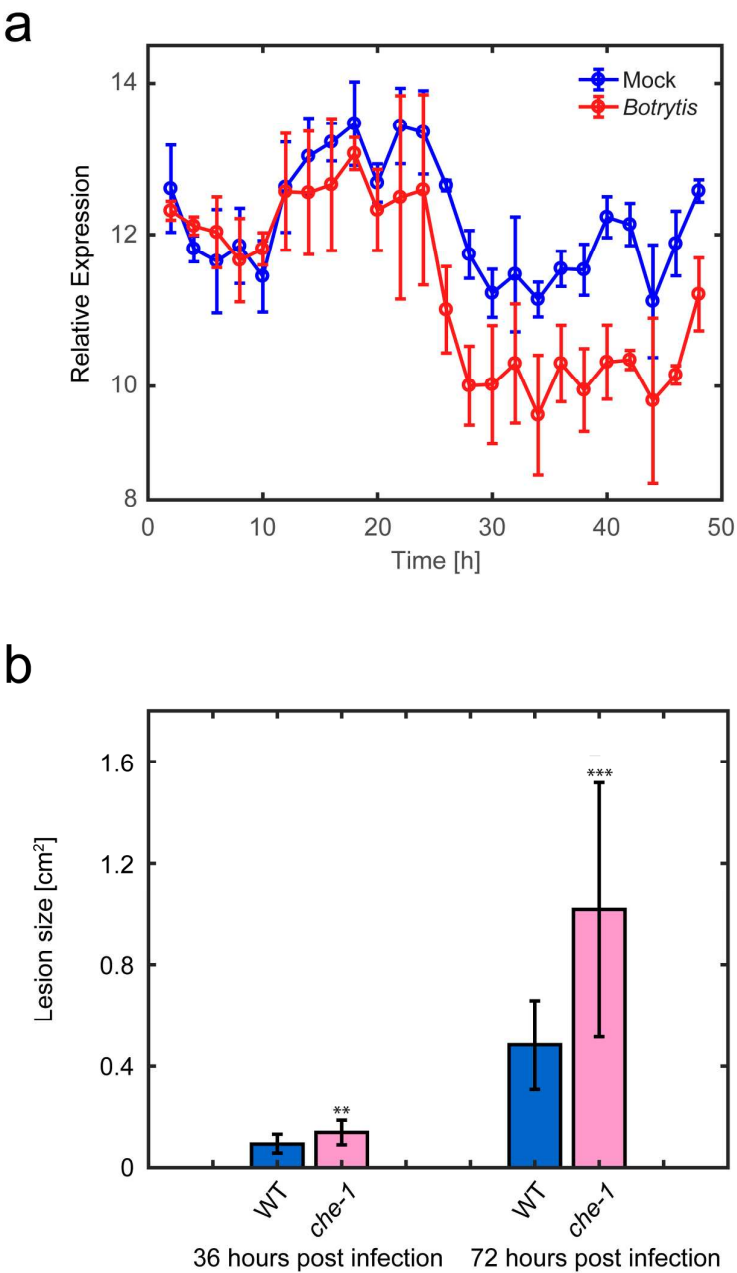


**Figure 1.** Expression and role of CHE during infection with *B. cinerea* (a) Expression of the TF CHE is downregulated during *B. cinerea* infection of Arabidopsis leaves. Leaves were drop-inoculated with *B. cinerea* spores or mock-inoculated, and genome-wide gene expression determined every 2 hours for both mock treatment (blue) and *B. cinerea* infection (red). Open circles are the average of four biological repeats with bars representing standard deviation. This data is extracted from Windram et al.<sup>10</sup> (b) CHE is a positive regulator of defence against *B. cinerea*. Lesion size of Arabidopsis leaves ( $n = 17$ ) drop-inoculated with *B. cinerea* spores were measured 36 and 72 hours post infection. *che-1* is an Arabidopsis

mutant with significantly reduced *CHE* expression. WT is the wildtype Col-0 Arabidopsis accession. Error bars represent standard deviation, \*\* represents  $p \leq 0.01$  and \*\*\* represents  $p \leq 0.001$ .

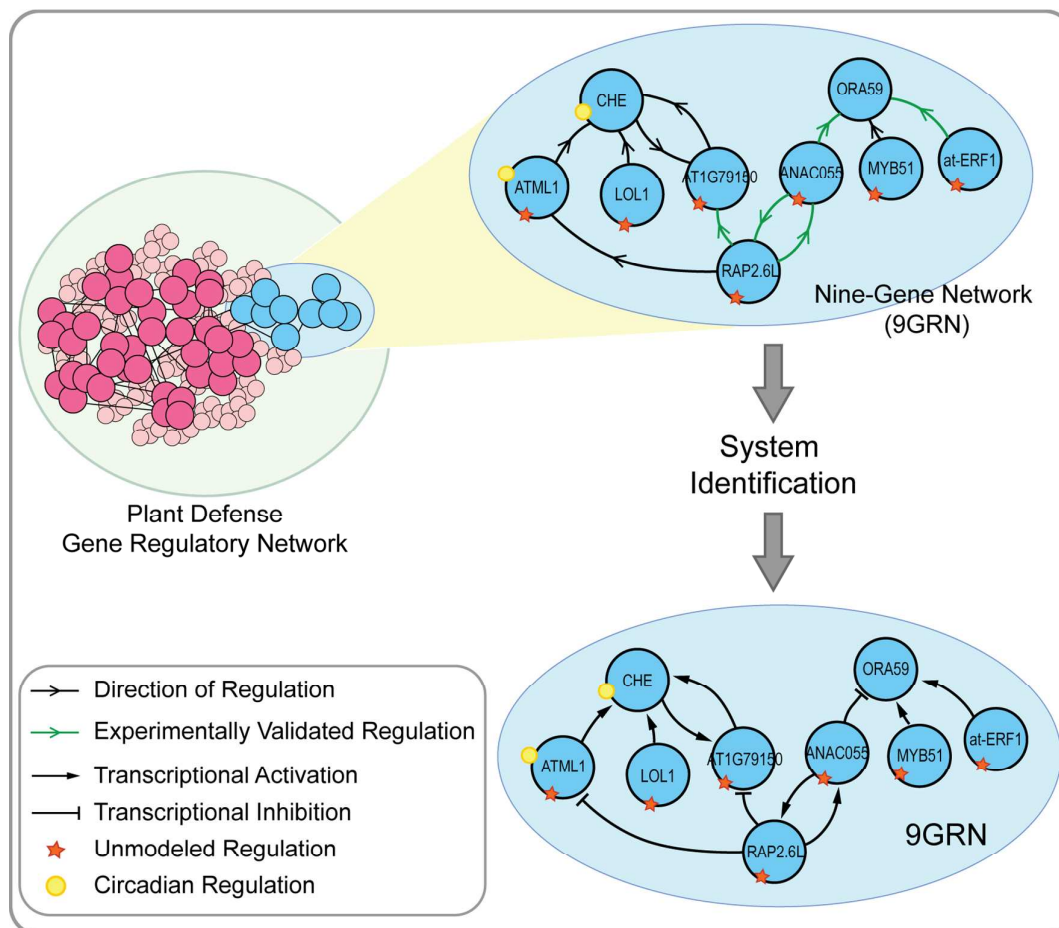


**Figure 2.** Network model of gene regulatory events mediating transcriptional response to *Botrytis cinerea*. The nine-gene network (9GRN) is a sub-network of the initial network model inferred from time series transcriptome data. The direction of regulation is indicated by the arrow. Red stars represent unmodeled regulation (e.g. direct regulation from *B. cinerea*, noise and other unidentified regulation, see also Section S5 of the Supporting Information). The yellow circle represents circadian regulation. Green edges represent interactions that are supported by experimental data. The regulation types (arrow-head and bar-head) in 9GRN are identified through system identification.

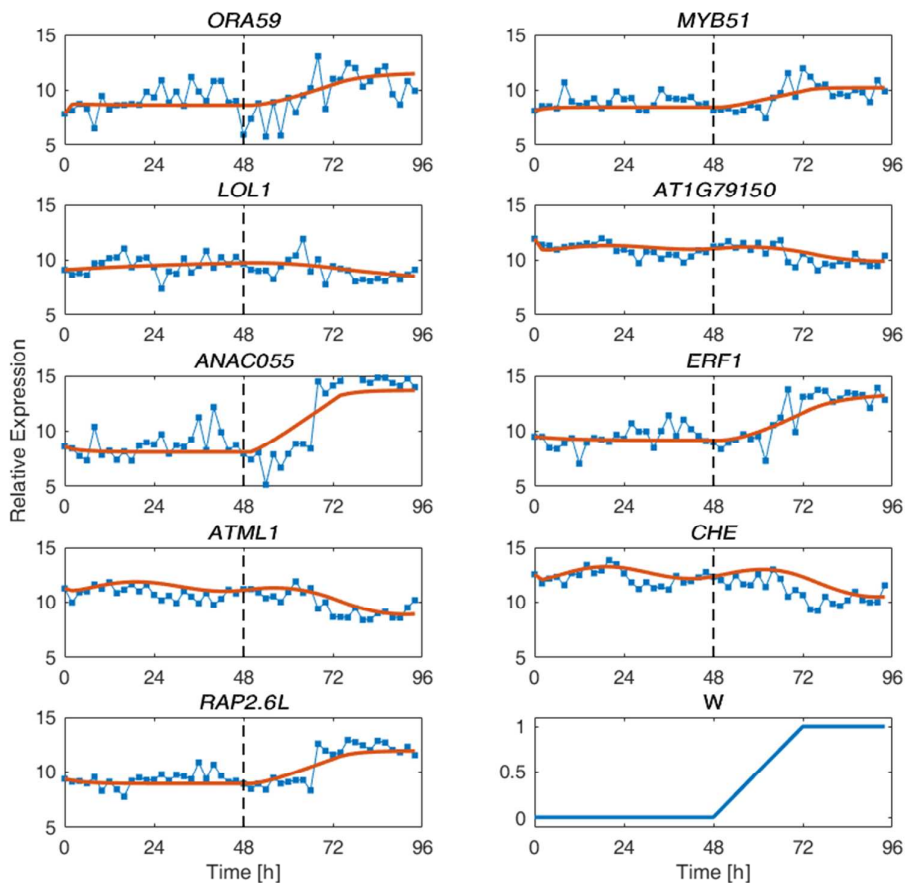


**Figure 3.** Validation of the linear model against an experimental data set that was not used in the parameter estimation exercise. The experimental data sets in ref 10 are composed of two time series, one mock-inoculated and one *B. cinerea*-inoculated. Here, these two time series are joined (denoted by the vertical dashed line) to illustrate a transition from pre- to post-infection, with *B. cinerea* infection starting at time 48 hours. There are four sets of such joined time-series data; we used the average of the first three data sets for parameter estimation (see Figure S3), leaving the fourth data set for model validation shown above. We have also included the unmodeled regulation, W described by Equation S5.1. Line with dots: Experiment data, Solid line: Linear model.

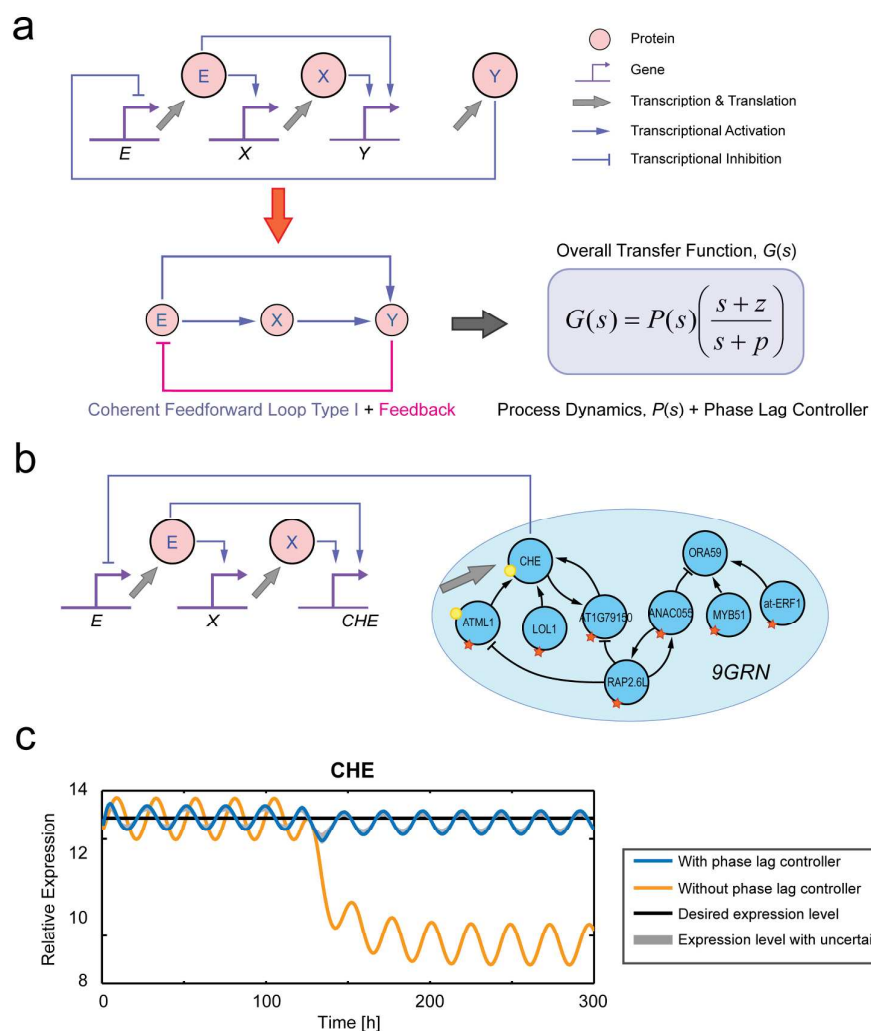


**Figure 4.** Perturbation mitigation using a genetic phase lag controller. (a) Genetic circuit of the proposed controller. *X* is the output of the controller, *Y* is the output of the process and *E* computes the error signal. This genetic circuit is equivalent to a coherent feedforward loop type-I with feedback network motif that yields the transfer function of a phase lag controller plus process dynamics. (b) Implementation of the phase lag controller motif for perturbation mitigation in the 9GRN. (c) Simulation results of phase lag controller in mitigating perturbation in the 9GRN. The solid black line is the desired average expression of *CHE*, the solid yellow line is the expression of *CHE* during infection with *B. cinerea* without any control action, and the solid blue lines represent gene expression during infection with *B. cinerea* with control action. The gray shaded regions represent the expression level with uncertainty obtained through Monte Carlo simulation. In our simulations, the parameter values for the phase lag controller are  $\alpha_{X,E} = 3.00$ ,  $\alpha_{Y,X} = 5.00$ ,  $\alpha_{Y,E} = 5.00$ ,  $\beta_X = 0.026$ , while the parameter values for the error computation are  $b_{S,E} = 6.21$  and  $\gamma = \beta_E = 0.50$ . For more details on the choice of these values, see Figures S6 to S8.

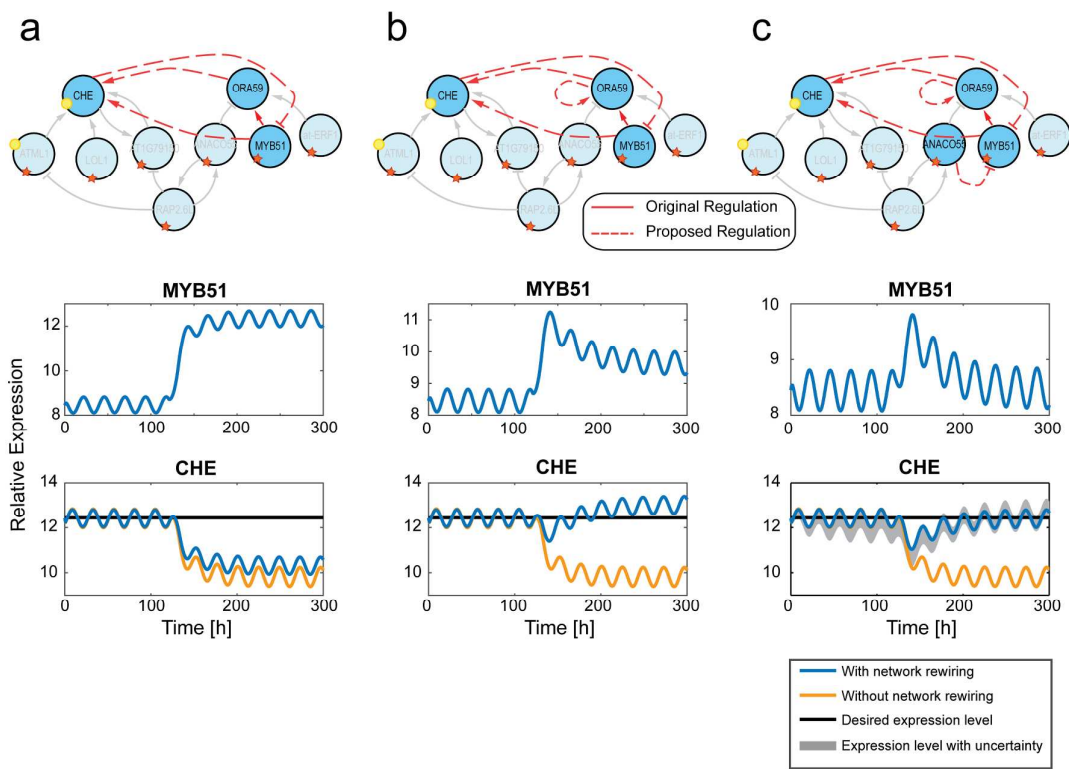


**Figure 5.** Simulation results for genes in the 9GRN with proposed network rewiring. Black line: reference value, Blue line: gene expression level in response to *B. cinerea* infection after rewiring. Yellow line: gene expression level in response to *B. cinerea* infection without network rewiring. Perturbation (inoculation) is given at time 120 hours. (a) Rewiring a controller by adding activation of CHE by MYB51 and ORA59 and inhibition of MYB51 expression by CHE. (b) Addition of positive autoregulation to ORA59. (c) Addition of feedforward component; inhibition of MYB51 by ANAC055. The gray shaded regions represent the expression level with uncertainty obtained through Monte Carlo simulation.

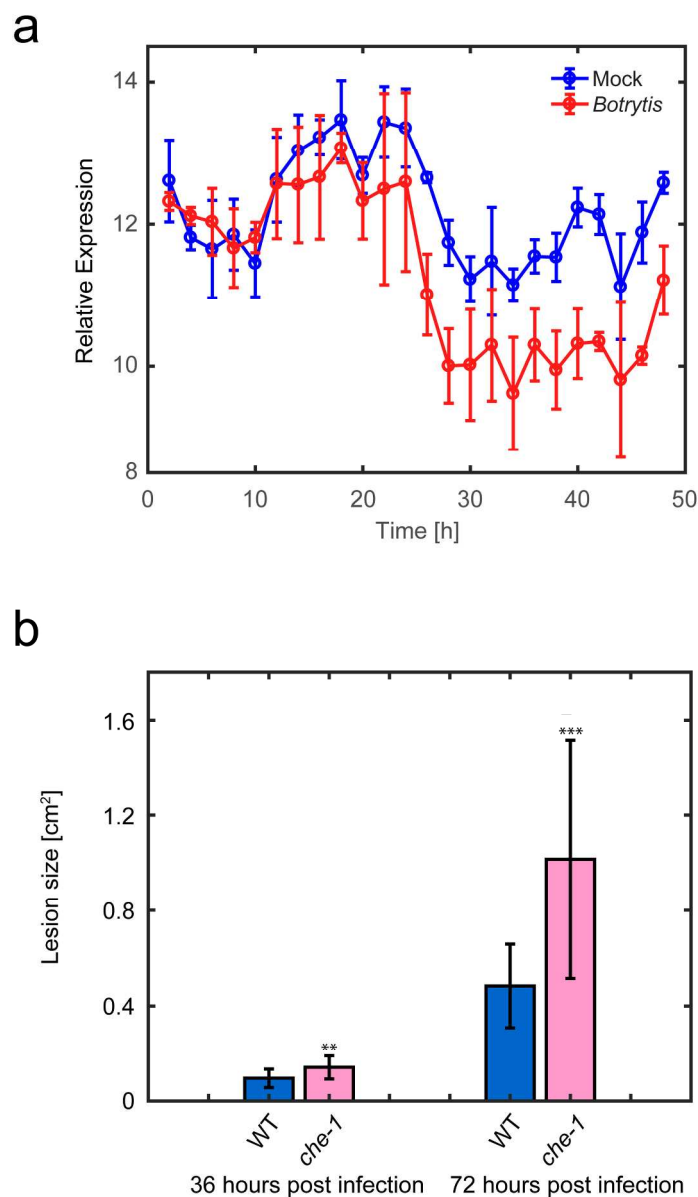


Figure 1. Expression and role of CHE during infection with *B. cinerea* (a) Expression of the TF CHE is downregulated during *B. cinerea* infection of *Arabidopsis* leaves. Leaves were drop-inoculated with *B. cinerea* spores or mock-inoculated, and genome-wide gene expression determined every 2 hours for both mock treatment (blue) and *B. cinerea* infection (red). Open circles are the average of four biological repeats with bars representing standard deviation. This data is extracted from Windram et al.<sup>10</sup> (b) CHE is a positive regulator of defence against *B. cinerea*. Lesion size of *Arabidopsis* leaves ( $n = 17$ ) drop-inoculated with *B. cinerea* spores were measured 36 and 72 hours post infection. *che-1* is an *Arabidopsis* mutant with significantly reduced CHE expression. WT is the wildtype Col-0 *Arabidopsis* accession. Error bars represent standard deviation, \*\* represents  $p \leq 0.01$  and \*\*\* represents  $p \leq 0.001$ .

145x254mm (300 x 300 DPI)



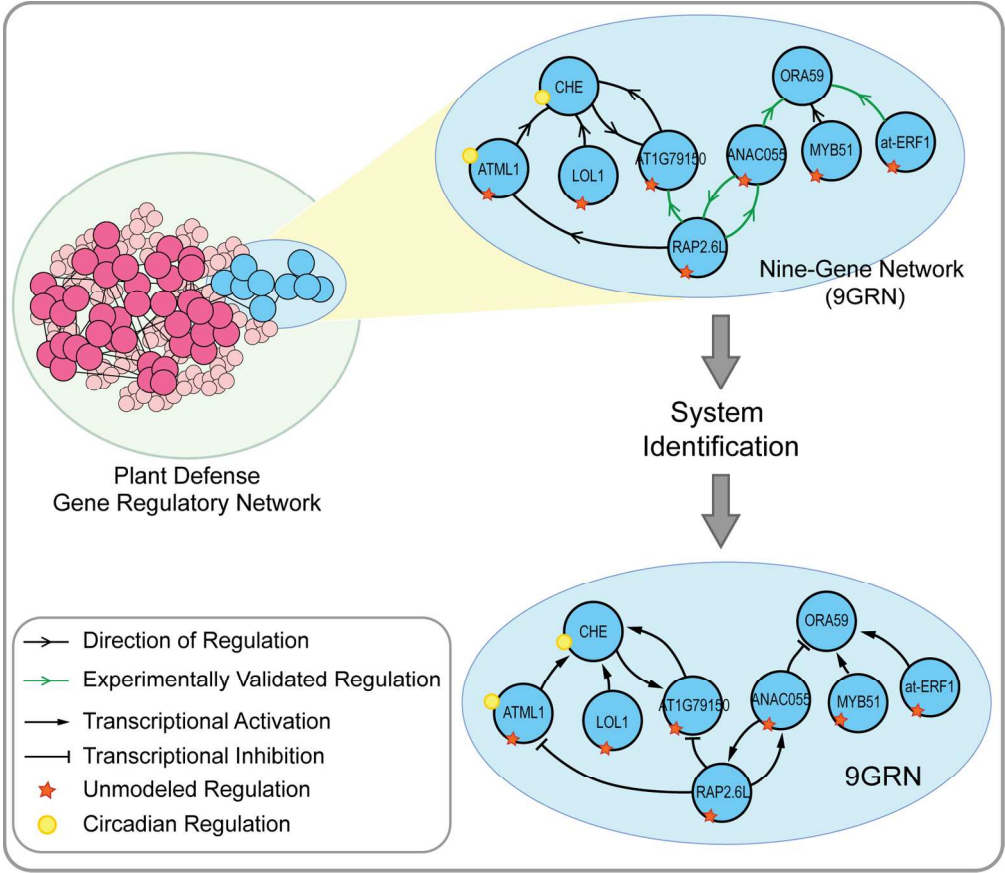


Figure 2. Network model of gene regulatory events mediating transcriptional response to *Botrytis cinerea*. The nine-gene network (9GRN) is a sub-network of the initial network model inferred from time series transcriptome data. The direction of regulation is indicated by the arrow. Red stars represent unmodeled regulation (e.g. direct regulation from *B. cinerea*, noise and other unidentified regulation, see also Section S5 of the Supporting Information). The yellow circle represents circadian regulation. Green edges represent interactions that are supported by experimental data. The regulation types (arrow-head and bar-head) in 9GRN are identified through system identification.

151x131mm (300 x 300 DPI)

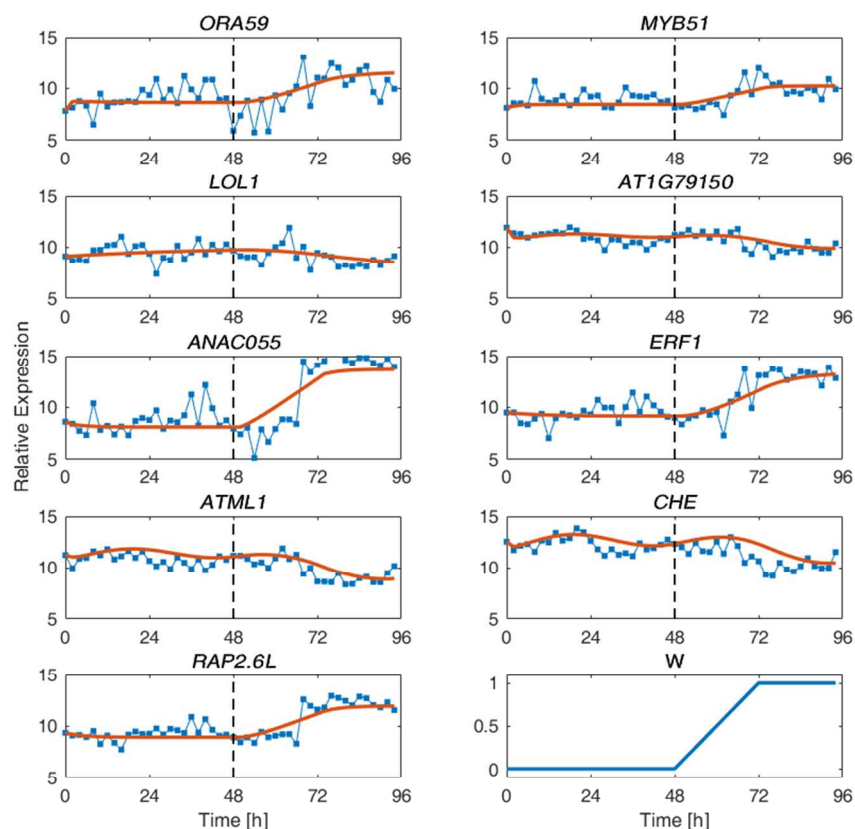


Figure 3. Validation of the linear model against an experimental data set that was not used in the parameter estimation exercise. The experimental data sets in ref 10 are composed of two time series, one mock-inoculated and one *B. cinerea*-inoculated. Here, these two time series are joined (denoted by the vertical dashed line) to illustrate a transition from pre- to post-infection, with *B. cinerea* infection starting at time 48 hours. There are four sets of such joined time-series data; we used the average of the first three data sets for parameter estimation (see Figure S3), leaving the fourth data set for model validation shown above. We have also included the unmodeled regulation, *W* described by Equation S5.1. Line with dots: Experiment data, Solid line: Linear model.

249x230mm (96 x 96 DPI)